



## Functional analysis of *MITF* gene mutations associated with Waardenburg syndrome type 2

Hua Zhang<sup>a,b,1</sup>, Hunjin Luo<sup>d,1</sup>, Hongsheng Chen<sup>a,c</sup>, Lingyun Mei<sup>a,c</sup>, Chufeng He<sup>a,c</sup>, Lu Jiang<sup>a,c</sup>, Jia-Da Li<sup>d,\*</sup>, Yong Feng<sup>a,c,d,\*</sup>

<sup>a</sup> Department of Otolaryngology, Xiangya Hospital, Central South University, Changsha, Hunan 410078, People's Republic of China

<sup>b</sup> Department of Otolaryngology, First Affiliated Hospital, Xinjiang Medical University, Urumqi, Xinjiang 830054, People's Republic of China

<sup>c</sup> Province Key Laboratory of Otolaryngology Critical Diseases, Changsha, Hunan 410008, People's Republic of China

<sup>d</sup> State Key Laboratory of Medical Genetics, Central South University, Changsha, Hunan 410078, People's Republic of China

### ARTICLE INFO

#### Article history:

Received 4 April 2012

Revised 17 September 2012

Accepted 5 October 2012

Available online 23 October 2012

Edited by Ulrike Kutay

#### Keywords:

Waardenburg syndrome

*MITF*

Mutation

Haploinsufficiency

### ABSTRACT

***MITF* mutations results in an abnormal melanocyte development and lead to Waardenburg syndrome type 2 (WS2). Here, we analyzed the *in vitro* activities of two recently identified WS2-associated *MITF* mutations (p.R217I and p.T192fsX18). The R217I *MITF* retained partial activity, normal DNA-binding ability and nuclear distribution, whereas the T192fsX18 *MITF* failed to activate *TYR* promoter and showed aberrant subcellular localization which may be caused by deletion of nuclear localization signal (NLS) at aa 213–218 (ERRRRF). These results suggest that haploinsufficiency may be the underlying mechanism for the mild phenotypes of WS2 caused by these two mutations.**

© 2012 Federation of European Biochemical Societies. Published by Elsevier B.V. All rights reserved.

## 1. Introduction

Microphthalmia-associated transcription factor (*MITF*), a basic helix–loop–helix leucine zipper (bHLHZip) transcription factor, plays a key role in survival and differentiation of melanocytes [1–4]. In melanocytes, *MITF* regulates the expression of major melanogenic genes such as tyrosinase (*TYR*), tyrosinase-related protein-1 (*TYRP1*), and tyrosinase-related protein-2 (*TYRP2*) [5,6]. *MITF* directly upregulates the expression of *TYR*, *TYRP1*,

and *TYRP2* by binding to the E-box motif (CANNTG) within the promoter [4,6–9]. These genes encode enzymes required for normal melanin synthesis in melanocytes [7,9,10]. The three enzymes, especially tyrosinase, are key players in the melanocyte differentiation, as demonstrated by the dramatic consequences of their mutations on melanin pigment production [11].

Some homozygous *Mitf* mutant mice can normally survive but are microphthalmic, deaf, and completely white due to lacking melanocytes [2,12], whereas some heterozygous *Mitf* mutant mice show the striking phenotype of belly spotting [13]. In human, *MITF* mutations are associated with ~15% of Waardenburg syndrome type 2 (WS2). Waardenburg syndrome (WS) is an autosomal dominantly inherited disorder of neural crest cells (NCC) characterized by sensorineural deafness and abnormal pigmentation of the hair, skin and iris [14]. Clinically, WS is divided into four types (WS1–4) based on the presence or absence of additional symptoms. WS2 is characterized as absence of additional features.

We previously reported two mutations c.650G>T (p.R217I) and c.575delC (p.T192fsX18) in the *MITF* gene in two different families with WS2 [15]. To understand the functional consequences of these mutations, we analyzed the subcellular distribution, expression and *in vitro* activities.

**Abbreviations:** DAPI, 4,6-diamino-2-phenylindole; DTT, 1,4-dithiothreitol; GFP, green fluorescence protein; *MITF*, microphthalmia-associated transcription factor; NLS, nuclear localization signal; NPC, nuclear pore complex; *TYR*, tyrosinase; *TYRP1*, tyrosinase-related protein-1; *TYRP2*, tyrosinase-related protein-2; WS, Waardenburg syndrome

\* Corresponding authors. Addresses: State Key Laboratory of Medical Genetics, Central South University, 110 Xiangya Road, Changsha, Hunan 410078, People's Republic of China. Fax: +86 731 84805339 (J.-D. Li), Department of Otolaryngology, Xiangya Hospital, Central South University, 87 Xiangya Road, Changsha, Hunan 410008, People's Republic of China. Fax: +86 731 89753545 (Y. Feng).

E-mail addresses: [lijia@sklmg.edu.cn](mailto:lijia@sklmg.edu.cn) (J.-D. Li), [fyong@xysm.net](mailto:fyong@xysm.net) (Y. Feng).

<sup>1</sup> These authors contributed equally to this work.

## 2. Materials and methods

### 2.1. Reporter and expression constructs

The luciferase reporter containing the human *TYR* promoter (pGL3-Tyr-Luc) and the expression constructs had been described previously and were kindly provided by Vachtenheim et al. [16]. To generate MITF tagged with 3×Flag at the N-terminus (Flag-MITF), full length *MITF* cDNA (GenBank Accession No.: NM\_000248.2) was amplified from pCMV-MITF-HA and subcloned into pCMV-3×Flag (Sigma, St. Louis, WA, USA). The R217I MITF, T192fsX18 MITF and MITF lacking NLS (MITFΔNLS) were generated by using QuikChange II Site-Directed Mutagenesis (GE Healthcare, Chalfont St. Giles, Buckinghamshire, UK). Further, a synthetic oligonucleotide encoding the NLS (ERRRRF) of MITF was cloned into pEGFP-N1 (Sigma) at EcoRI/BamHI site to add a NLS to the N-terminus of GFP. All constructs were verified by direct nucleotide sequencing.

### 2.2. Cell culture, transfections, and luciferase reporter assays

The melanoma UACC903 cells or NIH3T3 cells were grown at 37 °C under 5% CO<sub>2</sub> in Dulbecco's modified Eagle medium (DMEM) supplemented with 10% fetal bovine serum (FBS) and 100 U/ml of penicillin/streptomycin as described [17]. Twenty-four hours before transfection, melanoma UACC903 cells were seeded at an approximate 50% confluency in 24-well plates. Cells were transfected with 5 ng of the reporter plasmid and 20 ng of the expression plasmid, using Lipofectamine 2000 reagent (Invitrogen, Carlsbad, CA, USA) according to the manufacturer's protocol, and 5 ng of pCMV-β-gal (BD biosciences/Clontech, Palo Alto, CA, USA) was included for normalization of transfection efficiency. The final DNA amount of each well was adjusted to 200 ng with empty vectors. At 48 h after transfection, cells were washed with phosphate buffered saline (PBS) and lysed with Reporter Lysis Buffer (Promega, Madison, WI, USA). The extracts were assayed for luciferase and β-galactosidase activity. Luciferase reporter assays were performed using Luciferase Assay System (Promega) according to the manufacturer's protocol. Luciferase activities were determined using SIRIUS luminometer (Berthold Detection Systems GmbH, Pforzheim, Germany). As for competition assays, various amounts of mutant MITF plasmids (20, 40, 80 ng) were mixed with a fixed amount of WT MITF (20 ng) and the reporter *TYR* plasmid (5 ng) in the transfection. All reporter assays were conducted at least three times and performed in triplicate on different days using different batches of cells. Data were analyzed using Prism 4 software (GraphPad, Software Inc., San Diego, CA, USA).

### 2.3. Western blot analysis

The melanoma UACC903 cells were transfected with 200 ng of Flag-MITF or its mutant constructs using Lipofectamine 2000 reagent in 12-well plates. At 48 h after transfection, cells were lysed in 2× SDS loading buffer, containing 1 mM phenylmethanesulfonyl fluoride (PMSF) (Sigma), and 0.2 mM β-mercaptoethanol supplemented with protease inhibitor cocktail (Sigma). Proteins were separated on sodium dodecyl sulfate polyacrylamide gels (SDS-PAGE) and transferred onto a polyvinylidene fluoride (PVDF) membrane (Millipore, Billerica, MA, USA). The membrane was blocked in Tris-buffered saline supplemented with 5% non-fat milk for 1 h at room temperature and then incubated overnight at 4 °C with mouse monoclonal anti-Flag M2 antibody (1:1000 dilution, Sigma). After washing with Tris-buffered saline supplemented with 0.1% Tween 20 (Sigma), the membrane was incubated for 1 h at room temperature with a horseradish peroxidase-conjugated secondary

anti-mouse IgG antibody (1:10000 dilution, Sigma). Detection were performed using the ECL plus Western blotting detection system (GE Healthcare) according to manufacturer's instruction.

### 2.4. Biotinylated DNA affinity precipitation

The MITF-binding oligonucleotide derived from the promoter of human *TYR* gene, 5'-GAAAAGTCAGTCATGTCCTTTTCAG-3', and mutated DNA-binding probe 5'-GAAAAGTCAGTGTGCATCTTTTCAG-3' were biotinylated at the 5'-terminus, and then annealed with its complementary strand to generate WT and mutant double-stranded oligonucleotides, respectively. The melanoma UACC903 cells were transfected with Flag-MITF, Flag-R217I, or Flag-T192fsX18 using Lipofectamine 2000 reagent in six-well plates. Forty-eight hours after transfection, cells were lysed by sonication in HKMG buffer (10 mM HEPES, pH 7.9, 100 mM KCl, 5 mM MgCl<sub>2</sub>, 10% glycerol, 1 mM DTT, and 0.5% of Nonidet-P40) containing protease inhibitors. Cellular debris was removed by centrifugation. Ten percent cell lysates were extracted and added 2× SDS/0.2 mM β-mercaptoethanol for input immunoblotting. Remaining cell lysates were brought to a final volume of 1 ml and precleared with 30 μl streptavidin-agarose beads (Sigma) with rotation at 4 °C for 1 h, then incubated with or without 8 μg of biotinylated double-stranded oligonucleotide and 10 μg of poly(dI-dC).poly(dI-dC) (Sigma) with rotation at 4 °C for 20 h. Forty microliters streptavidin-agarose beads were added and samples were incubated for another 2 h at 4 °C. Beads/DNA/protein or beads/protein complexes were washed three times using cold ice HKMG buffer and resuspended in 2× SDS/0.2 mM β-mercaptoethanol. Samples were boiled at 95 °C for 10 min and subsequently separated on 12% SDS-PAGE. Anti-Flag M2 antibody was used in the subsequent immunoblotting.

### 2.5. Immunofluorescence assays

The melanoma UACC903 cells or NIH3T3 cells were plated on 24-well plates and transfected with 50 ng of each MITF constructs. At 48 h after transfection, cultures were fixed in 4% paraformaldehyde for 30 min at room temperature. After permeabilized for 1 h in PBS/0.2% Triton X-100 (Bio Basic Inc, Bailey Avenue Amherst, NY, USA), they were incubated with blocking solution (PBS, 3% bovine serum albumin, 5% goat serum) for 1 h. Incubation with primary anti-Flag M2 (1:600 dilution) was performed at 4 °C overnight. After washed with PBS/0.2% Triton X-100 three times, fluorescence-labeled secondary anti-mouse antibodies (1:300 dilution; Invitrogen) were incubated for 2 h in a dark room. After incubation of 4,6-diamino-2-phenylindole (DAPI; Invitrogen) for 3 min, cells were mounted in Fluoromount medium (Sigma) and fluorescence images were examined with a laser scanning confocal system installed on a Carl Zeiss microscope (Zeiss, Göttingen, Germany) with a 63× oil immersion objective. Images were analyzed using the Metaphor software package.

## 3. Results

### 3.1. Mutations of MITF in WS2

We previously identified two heterozygous mutations c.650G>T (p.R217I) and c.575delC (p.T192fsX18) in the *MITF* genes in three WS2 cases, presenting with deafness and heterochromia irides [15]. The p.R217I is a missense mutation found in the basic domain of bHLHZip region of exon 7, causing an arginine to isoleucine substitution at codon 217 (Fig. 1A). The p.T192fsX18 is a frameshift mutation which generates different sequences starting at position 192 in exon 6 and introduces a premature stop codon at position

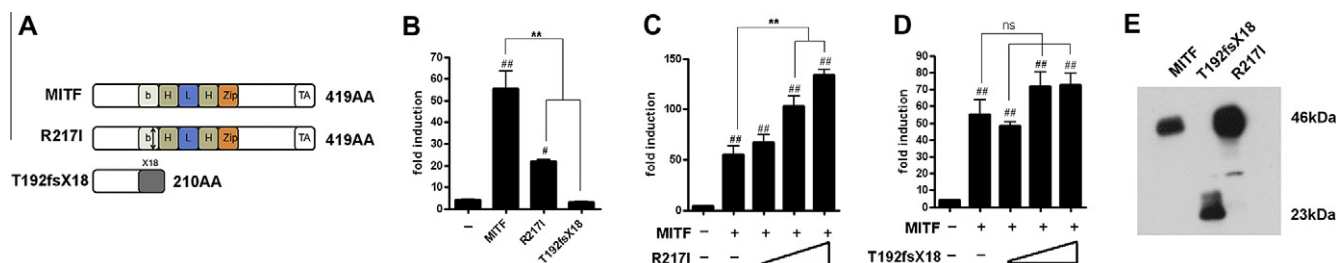


**Fig. 1.** Functional and Western blot analysis of WS-associated MITF proteins. (A) Schematic representation of the WT, R217I, and T192fsX18 MITF. The bHLH-Zip domain and C-terminal transcriptional activation (TA) domain are shown. R217I is missense mutant and the arrow indicates mutation site in basic domain. T192fsX18 is a frameshift mutant and the filled box represents resulting frameshift from mutation site to premature stop codon. (B) Transcriptional activities of MITF and its mutants determined by luciferase activity assays. The luciferase reporter plasmid Tyr-Luc were transiently transfected into melanoma UACC903 cells in combination with WT or mutant MITF expression plasmids. (C and D) Effect of R217I or T192fsX18 mutants on WT MITF transactivity. Increasing amounts of mutant R217I or T192fsX18 expression plasmids were cotransfected with a fixed amount of WT MITF expression plasmid and the luciferase reporter plasmid Tyr-Luc. For (B)–(D), the basal level of luciferase was set as 1. Data from all other transfections are presented as fold induction above this level. Luciferase activity was normalized by measuring  $\beta$ -galactosidase activity. Each value shown was the mean  $\pm$  SEM of three replicates from a single assay. The results shown were representative of at least three independent experiments. (E) Melanoma UACC903 cells were transiently transfected with plasmids expressing either the WT or mutant variants of MITF. Proteins from whole cell lysates were analyzed by SDS-PAGE (12%) and the expression of MITF was visualized using monoclonal antibody against Flag epitope (\* $P$  < 0.05, \*\* $P$  < 0.01, as compared with the basal activity; \*\* $P$  < 0.01, as compared with the WT; ns, not significant; unpaired Student's  $t$ -test).

210 (Fig. 1A), resulting in truncated protein without bHLHZip domain and transactivation domain.

### 3.2. Transcriptional activities of mutant MITFs

MITF can induce the transcription of target gene *TYR* and subsequently the expression of the melanocyte-specific enzyme tyrosinase [7,18]. A luciferase reporter construct containing the *TYR* promoter sequences was used to study if diseases-associated mutations affected MITF activity. As shown in Fig. 1B, WT MITF was able to increase the *TYR* promoter activity by about 55-fold, consistent with previous reports [16–19]. However, the transactivity of R217I MITF was dramatically reduced as compared with WT, whereas the T192fsX18 mutant failed to transactivate the *TYR* promoter, indicating that R217I mutant was partially functional while T192fsX18 mutant was loss-of-function.

Some loss-of-function mutant proteins may compete with their WT protein binding to the promoter of target genes and inhibit the activity of WT proteins, i.e. dominant negative effect. To determine whether the R217I and T192fsX18 MITF were able to interfere with WT MITF function, we carried out competition assays by cotransfecting WT and R217I or T192fsX18 MITF expression plasmids together with the reporter plasmid. The *TYR* promoter activity induced by WT MITF was increased with the addition of R217I, consistent with its residual (~50%) activity. T192fsX18 did not show significant effect on the transcriptional activity of WT MITF (Fig. 1C and D).

### 3.3. Exogenous expression of MITF proteins

To investigate whether the disrupted function is caused by the expression level of mutant MITF, we performed Western blot analysis on protein extracts from melanoma UACC903 cells transfected with WT, R217I, or T192fsX18 MITF plasmid. As shown in Fig. 1E, both WT and mutant MITF proteins were detected at the expected size. There was no apparent difference between WT and mutant MITF in the expression level.

### 3.4. DNA binding capacity of MITF mutants

To determine the DNA-binding capacity of WT and mutant MITFs, we used a biotinylated double-stranded oligonucleotide containing MITF binding sequence to precipitate proteins from UACC903 cells transfected with WT, T192fsX18, or R217I MITF plasmids. As shown in Fig. 2, WT and R217I MITFs were able to

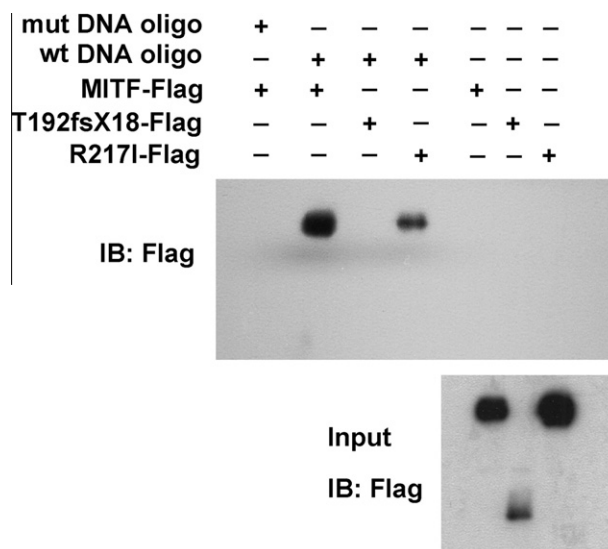


**Fig. 2.** DNA binding capacity of WS-associated MITF. The lysates of NIH3T3 cells transfected with WT, R217I, and T192fsX18 MITF plasmids were incubated with or without biotinylated double-stranded oligonucleotides of the MITF binding region at the *TYR* promoter. And the DNA/protein complex was pulled down with streptavidin-agarose beads. The precipitated proteins were separated on SDS-PAGE and analyzed by immunoblotting using anti-Flag M2 antibody. DNA precipitation demonstrates that R217I mutant retains the DNA-binding activity, whereas T192fsX18 mutant lose capability to bind to DNA. As a negative control, WT MITF protein did not bind to mutated double-stranded oligonucleotides.

bind specifically to the double-stranded DNA, consistent with their transcriptional activity. T192fsX18 MITF lacks the bHLHZip DNA-binding domain, thus was unable to bind the DNA. The WT MITF protein was not able to bind a double-stranded oligonucleotide with mutation in the E-box region, indicating the specificity of DNA-binding (Fig. 2).

### 3.5. Subcellular distribution of WT and mutant MITF proteins

As a transcription factor, MITF is localized in the nucleus. Then, we attempted to investigate if mutations altered the subcellular distribution of MITF protein by using immunofluorescence. As shown in Fig. 3, WT and R217I MITF were only localized in the nucleus, whereas T192fsX18 MITF was only localized in the cytoplasm. These results indicated that WT and R217I MITF produced

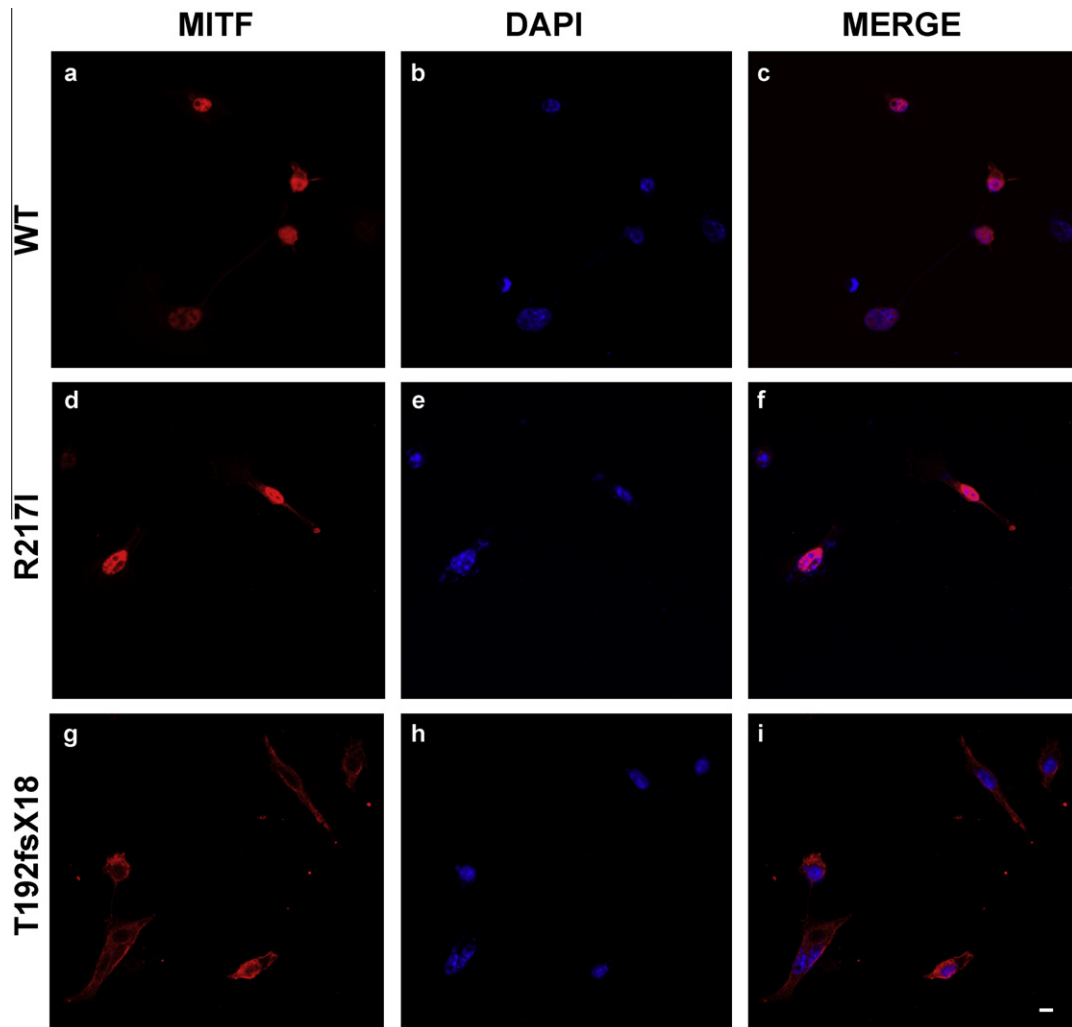


**Fig. 3.** Subcellular localization of WS-associated MITF proteins and T192fsX18-NLS in melanoma UACC903 cells. WT MITF and its mutant proteins (a, d, g) were shown in red, DAPI (b, e, h) revealing nucleus was shown in blue, and the merged images (c, f, i) were shown. Scale bar: 5  $\mu$ m.

in melanoma UACC903 cells were normally transported into nuclei, while T192fsX18 MITF was defective in the nuclear translocation.

### 3.6. Functional analysis of nuclear localization signal of MITF

Protein localized in nucleus contains specific nuclear localization signal (NLS) and can be recognized by transport protein to cross nuclear pore complex (NPC) into nucleus to exert its function. We speculate that the abnormal cytoplasmic distribution of T192fsX18 MITF may due to its loss of NLS. Indeed, MITF contains a putative NLS (NLIERRRRFNIN) between aa 210–221 at the C-terminal basic domain [19] (<http://cubic.bioc.columbia.edu/predictNLS/>). To examine whether this NLS is necessary for the MITF function, we made a MITF lacking of aa 213–218 (i.e. MITF $\Delta$ NLS). As shown in Fig. 4A, MITF $\Delta$ NLS failed to transactivate the *TYR* promoter. Importantly, the MITF $\Delta$ NLS protein was localized exclusively in the cytoplasm (Fig. 4B).

To examine whether this NLS sequences of MITF is sufficient to render cytoplasmic protein into nuclei, we tagged the NLS sequence of MITF (ERRRRF) to the N-terminus of green fluorescence protein (GFP). After transfected into the NIH3T3 cells, about 15% WT GFP was distributed in the nucleus, 30% was localized in the cytoplasm, whereas about 55% was seen in both cytoplasm and nucleus

(Fig. 4B and C). However, NLS-tagged GFP significantly increase the nuclei localization to about 80%, and about 18% of NLS-tagged GFP was observed in both cytoplasm and nuclei, while 2% of them was seen in the cytoplasm only (Fig. 4B and C).

## 4. Discussion

MITF encodes a 419-amino-acid transcription factor containing bHLHZip structure which is considered to bind DNA by the basic domain, to dimerize via the HLH domain, and to be stabilized by the Zip domain [1,2]. The carboxyl terminus of MITF contains a transcriptional activation domain and plays an important role in defining the target genes [8]. Tyrosinase is a key enzyme for melanin synthesis, which is encoded by the *TYR* gene, a melanocyte-specific gene. MITF binds to the specific E-box motif (CATGTG) within the promoter of *TYR* and initiates its transcription [7,8,18]. Few functional studies have been performed on human diseases-associated MITF mutations. Two non-sense mutations of MITF causing WS2 were shown to abrogate DNA binding and transactivation of the *TYR* promoter [17]. Another WS2-associated mutation, c.892T>C (p.S298P), impaired MITF function due to loss of the phosphorylation site by GSK3 $\beta$  [20]. We have shown here that WS2-associated T192fsX18 and R217I mutations attenuated the transactivity of MITF on *TYR* promoter.



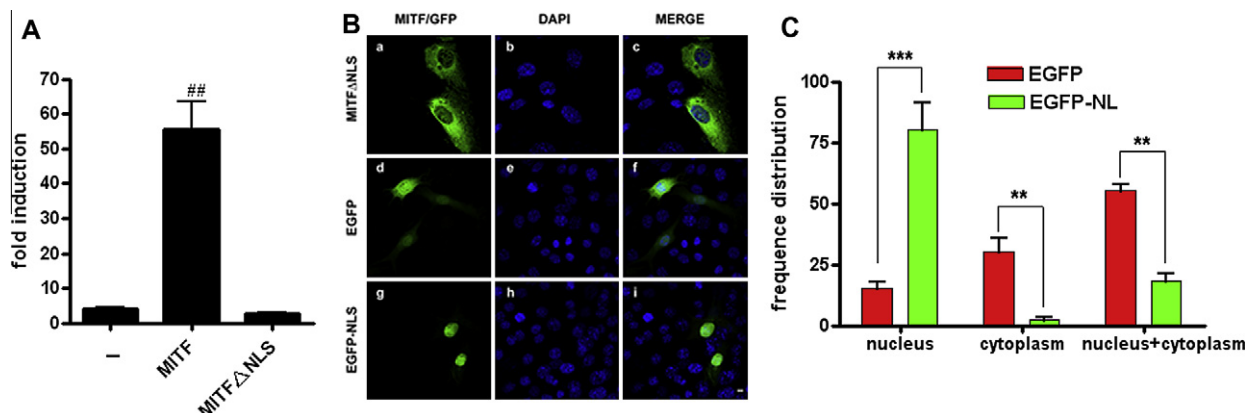


**Fig. 4.** Functional analysis of NLS of MITF. (A) Transcriptional activities of WT MITF and MITFΔNLS determined by luciferase activity assays. The luciferase reporter plasmid Tyr-Luc were transiently transfected into melanoma UACC903 cells in combination with WT MITF or MITFΔNLS expression plasmid. The basal level of luciferase was set as 1. Data from all other transfections are presented as fold induction above this level. Luciferase activity was normalized by measuring β-galactosidase activity. Each value shown was the mean ± SEM of three replicates from a single assay. The results shown were representative of at least three independent experiments (<sup>##</sup>*P* < 0.01, as compared with the basal activity, unpaired Student's *t*-test). (B) Subcellular localization of MITFΔNLS, EGFP, and EGFP-NLS in NIH3T3 cells was shown in green, DAPI revealing nucleus was shown in blue, and the merged images were shown. Scale bar: 5 μm. (C) Frequency distribution of GFP and GFP-NLS in transfected NIH3T3 cells (<sup>\*\*</sup>*P* < 0.01, <sup>\*\*\*</sup>*P* < 0.001, two-way ANOVA followed by Bonferroni tests).

The transactivity of R217I MITF was dramatically reduced as compared with WT, whereas the T192fsX18 mutant failed to transactivate the *TYR* promoter. Further, neither R217I nor T192fsX18 MITF showed dominant negative effect on the WT MITF, thus haploinsufficiency may be the underlying mechanism for WS2 pathogenesis. Similar results were obtained when non-melanocytic cell lines (human embryonic kidney 293 cells) were used (data not shown). Although only homozygous mice with null mutations showed apparent phenotype [21], MITF mutations were only identified in heterozygous forms in WS2 patients ([http://grenada.lumc.nl/LOVD2/WS/home.php?select\\_db=MITF](http://grenada.lumc.nl/LOVD2/WS/home.php?select_db=MITF)). In our cases, heterozygous T192fsX18 led to 50% reduction in the gene dosage; however, it should be noted that heterozygous R217I resulted in only ~25% reduction in the gene dosage. The different sensitivity of gene dosage between human and mice to MITF mutation may be a possible explanation. Nevertheless, as we only genotyped the known WS-related gene mutations in these patients, we cannot exclude the possibility that other unappreciated gene mutation, epigenetic effect or environmental factors may also contribute to the syndrome.

Protein localized in the nucleus frequently contains specific NLS that can be recognized by NLS-binding protein [22,23], and be transported through the nuclear pore into the nucleus. The basic domain of MITF may contain a NLS (210NLIERRRRFNIN221) [19] (<http://cubic.bioc.columbia.edu/predictNLS/>). The T192fsX18 mutant protein lacks NLS, which makes it not be recognized and transported into nucleus by NLS-binding protein, thus localized only in cytoplasm. Interestingly, we found T192fsX18 MITF distributed in both nucleus and cytoplasm in non-melanocytic NIH3T3 cell lines (data not shown), which may be due to its small molecular mass (predicted to be 23 kDa) to cross the nuclear pore complex via passive diffusion. The R217I mutation in the NLS did not impair the nuclear localization potential of MITF, consistent with the previous study [19,24]. They found that *Mitf*<sup>or</sup>-MITF encoded by the mouse *Mitf*<sup>or</sup> allele, with a R216K substitution in the basic domain, showed normal subcellular localization, suggesting that the nuclear translocation ability may not be affected by a substitution of one amino acid residue in NLS.

The function of MITF NLS was further demonstrated by loss-of-function and gain-of-function studies. In the loss-of-function study, MITF with deletion of NLS localized exclusively in the cytoplasm and failed to activate the *TYR* promoter. Conversely,

addition of this NLS to the N-terminus of GFP enhanced the translocation of GFP into nucleus.

In summary, we have shown that two recent identified WS2-associated mutations attenuated the transcriptional activity of MITF. As both mutations were in the heterozygous form and lack of dominant-negative effect, haploinsufficiency is the most reasonable mechanism, where the normal MITF protein resulted from one copy of the wild allele does not reach the threshold level necessary for full function of the protein.

### Conflict of interest

The authors declare that they have no conflict of interest.

### Acknowledgments

We would like to thank Jiri Vachtenheim for generously supplying the materials. This work was supported by the National Basic Research Program of China (2012CB517904), by grants from National Nature Science Foundation of China (30970958, 30971589, 81070481, 81170923 and 81260160) and by Youth Science Foundation Projects of Central South University (2012QNZT117). J.D.L. is a recipient of Lotus Scholar Professorship from Hunan Province, China.

### References

- [1] Hughes, M.J., Lingrel, J.B., Krakowsky, J.M. and Anderson, K.P. (1993) A helix-loop-helix transcription factor-like gene is located at the *mi* locus. *J. Biol. Chem.* 268, 20687–20690.
- [2] Hodgkinson, C.A., Moore, K.J., Nakayama, A., Steingrimsson, E., Copeland, N.G., Jenkins, N.A. and Arnheiter, H. (1993) Mutations at the mouse microphthalmia locus are associated with defects in a gene encoding a novel basic-helix-loop-helix-zipper protein. *Cell* 74, 395–404.
- [3] Tachibana, M., Perez-Jurado, L.A., Nakayama, A., Hodgkinson, C.A., Li, X., Schneider, M., Miki, T., Fex, J., Francke, U. and Arnheiter, H. (1994) Cloning of MITF, the human homolog of the mouse microphthalmia gene and assignment to chromosome 3p14.1–p12.3. *Hum. Mol. Genet.* 3, 553–557.
- [4] Hemesath, T.J., Steingrimsson, E., McGill, G., Hansen, M.J., Vaught, J., Hodgkinson, C.A., Arnheiter, H., Copeland, N.G., Jenkins, N.A. and Fisher, D.E. (1994) Microphthalmia, a critical factor in melanocyte development, defines a discrete transcription factor family. *Genes Dev.* 8, 2770–2780.
- [5] Yang, S.H., Han, J.S., Baek, S.H., Kwak, E.Y., Kim, H.J., Shin, J.H., Chung, B.H. and Kim, E.K. (2008) Construction of protein chip to detect binding of Mitf protein (microphthalmia transcription factor) and E-box DNA. *Appl. Biochem. Biotechnol.* 151, 273–282.

- [6] Goding, C.R. (2000) Mitf from neural crest to melanoma: signal transduction and transcription in the melanocyte lineage. *Genes Dev.* 14, 1712–1728.
- [7] Bentley, N.J., Eisen, T. and Goding, C.R. (1994) Melanocyte-specific expression of the human tyrosinase promoter: activation by the microphthalmia gene product and role of the initiator. *Mol. Cell. Biol.* 14, 7996–8006.
- [8] Yasumoto, K., Yokoyama, K., Takahashi, K., Tomita, Y. and Shibahara, S. (1997) Functional analysis of microphthalmia-associated transcription factor in pigment cell-specific transcription of the human tyrosinase family genes. *J. Biol. Chem.* 272, 503–509.
- [9] Bertolotto, C., Busca, R., Abbe, P., Bille, K., Aberdam, E., Ortonne, J.P. and Ballotti, R. (1998) Different cis-acting elements are involved in the regulation of TRP1 and TRP2 promoter activities by cyclic AMP: pivotal role of M boxes (GTCATGTGCT) and of microphthalmia. *Mol. Cell. Biol.* 18, 694–702.
- [10] Lowings, P., Yavuzer, U. and Goding, C.R. (1992) Positive and negative elements regulate a melanocyte-specific promoter. *Mol. Cell. Biol.* 12, 3653–3662.
- [11] Cheli, Y., Ohanna, M., Ballotti, R. and Bertolotto, C. (2010) Fifteen-year quest for microphthalmia-associated transcription factor target genes. *Pigment Cell Melanoma Res.* 23, 27–40.
- [12] Steingrimsson, E., Moore, K.J., Lamoreux, M.L., Ferre-D'Amare, A.R., Burley, S.K., Zimring, D.C., Skow, L.C., Hodgkinson, C.A., Arnheiter, H. and Copeland, N.G. (1994) Molecular basis of mouse microphthalmia (mi) mutations helps explain their developmental and phenotypic consequences. *Nat. Genet.* 8, 256–263.
- [13] Hou, L. and Pavan, W.J. (2008) Transcriptional and signaling regulation in neural crest stem cell-derived melanocyte development: do all roads lead to Mitf? *Cell Res.* 18, 1163–1176.
- [14] Read, A.P. and Newton, V.E. (1997) Waardenburg syndrome. *J. Med. Genet.* 34, 656–665.
- [15] Chen, H., Jiang, L., Xie, Z., Mei, L., He, C., Hu, Z., Xia, K. and Feng, Y. (2010) Novel mutations of PAX3, MITF, and SOX10 genes in Chinese patients with type I or type II Waardenburg syndrome. *Biochem. Biophys. Res. Commun.* 397, 70–74.
- [16] Vachtenheim, J., Novotna, H. and Ghanem, G. (2001) Transcriptional repression of the microphthalmia gene in melanoma cells correlates with the unresponsiveness of target genes to ectopic microphthalmia-associated transcription factor. *J. Invest. Dermatol.* 117, 1505–1511.
- [17] Nobukuni, Y., Watanabe, A., Takeda, K., Skarka, H. and Tachibana, M. (1996) Analyses of loss-of-function mutations of the MITF gene suggest that haploinsufficiency is a cause of Waardenburg syndrome type 2A. *Am. J. Hum. Genet.* 59, 76–83.
- [18] Yasumoto, K., Yokoyama, K., Shibata, K., Tomita, Y. and Shibahara, S. (1994) Microphthalmia-associated transcription factor as a regulator for melanocyte-specific transcription of the human tyrosinase gene. *Mol. Cell. Biol.* 14, 8058–8070.
- [19] Takebayashi, K., Chida, K., Tsukamoto, I., Morii, E., Munakata, H., Arnheiter, H., Kuroki, T., Kitamura, Y. and Nomura, S. (1996) The recessive phenotype displayed by a dominant negative microphthalmia-associated transcription factor mutant is a result of impaired nucleation potential. *Mol. Cell. Biol.* 16, 1203–1211.
- [20] Takeda, K., Takemoto, C., Kobayashi, I., Watanabe, A., Nobukuni, Y., Fisher, D.E. and Tachibana, M. (2000) Ser298 of MITF, a mutation site in Waardenburg syndrome type 2, is a phosphorylation site with functional significance. *Hum. Mol. Genet.* 9, 125–132.
- [21] Zimring, D.C., Lamoreux, M.L., Millichamp, N.J. and Skow, L.C. (1996) Microphthalmia cloudy-eye (mi(ce)): a new murine allele. *J. Hered.* 87, 334–338.
- [22] Dingwall, C. and Laskey, R.A. (1991) Nuclear targeting sequences – a consensus? *Trends Biochem. Sci.* 16, 478–481.
- [23] Garcia-Bustos, J., Heitman, J. and Hall, M.N. (1991) Nuclear protein localization. *Biochim. Biophys. Acta* 1071, 83–101.
- [24] Kim, D.K., Morii, E., Ogiwara, H., Lee, Y.M., Jippo, T., Adachi, S., Maeyama, K., Kim, H.M. and Kitamura, Y. (1999) Different effect of various mutant MITF encoded by mi, Mior, or Miwh allele on phenotype of murine mast cells. *Blood* 93, 4179–4186.